HHS Public Access

Author manuscript

J Neurochem. Author manuscript; available in PMC 2016 May 01.

Published in final edited form as:

J Neurochem. 2015 May ; 133(4): 522–531. doi:10.1111/jnc.13059.

Kinetic diversity of dopamine transmission in the dorsal striatum

I. Mitch Taylor[1], **Kathryn M. Nesbitt**[1], **Seth H. Walters**[1], **Erika L. Varner**[1], **Zhan Shu**[1], **Kathleen M. Bartlow**[2], **Andrea S. Jaquins-Gerstl**[1], and **Adrian C. Michael**[1,*]

[1] Department of Chemistry, University of Pittsburgh, Pittsburgh, PA 15260, USA

[2] Department of Neurobiology, University of Pittsburgh, Pittsburgh, PA 15260, USA (current address: Earlham College, Department of Biology, 801 National Road West, Richmond, IN 47374)

Abstract

Dopamine (DA), a highly significant neurotransmitter in the mammalian central nervous system, operates on multiple time scales to affect a diverse array of physiological functions. The significance of DA in human health is heightened by its role in a variety of pathologies. Voltammetric measurements of electrically evoked dopamine release have brought to light the existence of a patchwork of DA kinetic domains in the dorsal striatum of the rat. Thus, it becomes necessary to consider how these domains might be related to specific aspects of DA's functions. Responses evoked in the fast and slow domains are distinct in both amplitude and temporal profile. Herein we report that responses evoked in fast domains can be further classified into four distinct types, types 1-4. The dorsal striatum, therefore, exhibits a total of at least five distinct evoked responses (4 fast types and 1 slow type). All five response types conform to kinetic models based entirely on first order rate expressions, which indicates that the heterogeneity among the response types arises from kinetic diversity within the dorsal striatum terminal field. We report also that functionally distinct sub-regions of the dorsal striatum express DA kinetic diversity in a selective manner. Thus, this study documents five response types, provides a thorough kinetic explanation for each of them, and confirms their differential association with functionally distinct sub-regions of this key DA terminal field.

Keywords

dopamine; domains; evoked release; voltammetry; dorsal striatum

INTRODUCTION

Dopamine (DA) is a highly significant neurotransmitter in the mammalian central nervous system that contributes to a diverse array of physiological functions, including motor control, sexual arousal, and reward (Hull et al., 1999, Brooks, 2001, Urban et al., 2012).

* Corresponding author: amichael@pitt.edu, (412) 624-8560.

There are no conflicts of interest.

DA's significance is heightened by its role in a number of pathologies that adversely affect human health, including Parkinson's disease, Alzheimer's disease, and schizophrenia (Pappata et al., 2008, de la Fuente-Fernandez et al., 2011, Kim et al., 2011). Evidence attributing DA's diversity of function and dysfunction to its ability to operate on multiple time scales (Grace, 1991, Schultz, 2007) establishes the importance of understanding the kinetics of processes that affect DA transmission, including DA release, clearance, and mass transport in the extracellular space. Fast scan cyclic voltammetry (FSCV) paired with electrical stimulation of DA axons in the medial forebrain bundle (MFB) is a well-established experimental paradigm for investigating these issues (Michael and Wightman, 1999).

FSCV paired with MFB stimulation has produced evidence that the rat dorsal striatum (DS) is organized as a patchwork of distinct DA kinetic domains (Moquin and Michael, 2009, Wang et al., 2010, Moquin and Michael, 2011, Taylor et al., 2012, Taylor et al., 2013). The patchwork comprises fast and slow domains that exhibit differences in the amplitude and temporal profile of evoked DA responses. In fast domains the responses rise immediately when the stimulus begins and then exhibit short-term depression (a decrease in the rate of ascension of the response as the stimulus continues). In slow domains the responses exhibit an initial delay, or lag, when the stimulus begins and then exhibit short-term facilitation (an increase in the rate of ascension of the response as the stimulus continues). Some responses are hybrids: they exhibit both short-term depression and facilitation.

Previous studies of the patchwork phenomenon have included extensive control experiments, which eliminate any possibility that the fast and slow responses are somehow due to the peculiarities of individual rats or individual voltammetric electrodes: likewise, evoked responses are not highly sensitive to the location of the stimulating electrode (Wagner et al., 2005, Shu et al., 2013). Instead, the recording site is the key factor in determining whether a response is fast, slow, or hybrid. Some earlier literature had attributed the heterogeneous features of the evoked responses to diffusional, and other, instrumental distortions (May and Wightman, 1989, Kawagoe et al., 1992). However, this view has undergone some revision due to the sensitivity of the response heterogeneity to several drugs (Moquin and Michael, 2009, Wang et al., 2010, Taylor et al., 2012). For example, the initial lag of the slow response had been attributed to a diffusion barrier. However, blockade of the dopamine transporter or of the D2 autoreceptor eliminates the initial lag of the slow response, revealing the presence of DA terminals in close proximity of slow recording sites. Such findings indicate that the initial lag is a kinetic, rather than diffusional, feature of the slow responses.

We report here that the fast domains produce four distinct types of evoked response (types 1-4). Thus, the DS produces at least five distinct responses, 4 fast types and 1 slow type. All five types may be reproduced with kinetic models based entirely on first order rate expressions. The models suggest that the five responses derive from local variations in DA kinetic parameters, while local diffusional variations play a relatively minor role. The models therefore attribute the heterogeneity of the evoked responses to kinetic diversity within the DA terminal field of the DS. The DS is a functionally heterogeneous structure (Crittenden and Graybiel, 2011, Smith and Graybiel, 2014), so we compared evoked DA

responses along two tracks in the medial and lateral DS. We show here that these functionally selective sub-regions of the DS are selective also with respect to DA kinetic diversity.

MATERIALS AND METHODS

Carbon fiber electrodes

Single carbon fibers (7-μm diameter, T650; Cytec Carbon Fibers LLC, Piedmont, SC, USA) were aspirated into borosilicate glass tubes (0.4 mm ID, 0.6 mm OD; A-M systems Inc., Sequim, WA, USA). The tubes were pulled to a fine tip around the fiber (Narishige puller, Los Angeles, CA, USA) and sealed with low viscosity epoxy (Spurr Epoxy; Polysciences Inc., Warrington, PA, USA). The exposed fibers were trimmed to a length of 200 μm. A droplet of mercury connected the fiber to a hookup wire (annealed nichrome; Goodfellow, Oakdale, PA, USA). The electrodes were soaked in isopropanol for at least 15 minutes prior to use (Bath et al., 2000).

Fast scan cyclic voltammetry

FSCV was performed under computer control (CV Tar Heels v4.3, courtesy of Dr. Michael Heien, University of Arizona, Tucson, AZ, USA) with an EI-400 potentiostat (Ensman Instruments, Bloomington, IN) or a locally built potential driver (Electronics Shop, Department of Chemistry, University of Pittsburgh) paired with a Keithley 428 current amplifier (Keithley Instruments, Cleveland, OH, USA). The resting potential for FSCV was 0 V vs. Ag/AgCl: the waveform comprised three potential sweeps (400 V/s) to +1.0 V, then to −0.5 V, and back to 0 V. The waveform repetition frequency was 10 Hz. DA was identified by inspection of color plots and background-subtracted cyclic voltammograms and quantified from the oxidation current measured between 0.5 and 0.7 V on the first potential sweep. Electrodes were calibrated in a flow cell using freshly prepared dopamine HCl (Sigma Aldrich, St. Louis, MO, USA) standards in N_2-purged artificial cerebrospinal fluid (142 mM NaCl, 1.2 mM $CaCl_2$, 2.7 mM KCl, 1.0 mM $MgCl_2$, 2.0 mM NaH_2PO_4, pH 7.4).

In vivo procedures

All procedures involving animals were approved by the University of Pittsburgh Institutional Animal Care and Use Committee. Male Sprague-Dawley rats (250-350 g, Hilltop Labs, Scottsdale, PA, USA) were anesthetized with isoflurane (2.5% by volume), placed in a stereotaxic frame, and wrapped in a 37°C blanket (Harvard Apparatus, Holliston, MA, USA). One or two (details below) carbon fiber electrodes were implanted into the DS and a stimulating electrode (bipolar stainless steel, MS303/a; Plastics One, Roanoke, VA, USA) was positioned over the MFB (2.2 mm posterior to bregma, 1.6 mm lateral from bregma, and 7-8.5 mm below the cortical surface, coordinates of (Pellegrino et al., 1979): the final vertical placement of the stimulating electrode was adjusted until evoked DA release was observed in the ipsilateral striatum (Ewing et al., 1983, Kuhr et al., 1984, Stamford et al., 1988). All experiments were performed in the right brain hemisphere. The stimulus was delivered via an optical isolation unit (Neurolog 800, Digitimer, Letchworth

Garden City, U.K.) and comprised a biphasic, constant-current, square wave (2 ms per pulse, 250 μA pulse height, 60 Hz frequency, 0.2 or 3 s duration).

Objective identification of fast and slow domains

As in previous studies (Moquin and Michael, 2009, Moquin and Michael, 2011, Taylor et al., 2012, Taylor et al., 2013), we objectively identified fast and slow recording sites by means of a brief test stimulus (60 Hz, 250 μA, 200 ms). Recording sites that respond to the test stimulus are classified as fast: otherwise, they are classified as slow. This conforms to the description of fast and slow sites given in the Introduction: fast sites respond immediately to the stimulus and slow sites exhibit initial lag. The responses reported below were evoked with the experimental stimulus selected for this work (60 Hz, 250 μA, 3 s).

Animals: kinetic diversity

To investigate DA's kinetic diversity we implanted 168 individual carbon fiber electrodes into the DS of 168 individual animals (a new electrode for each animal: 2.5 mm anterior to bregma, 2.5 mm lateral from bregma, and 5 mm below the cortical surface, coordinates of Pellegrino *et al*. 1979). The electrodes were stereotaxically lowered in 50-100 μm increments to a maximum depth of 6 mm below the cortical surface (the length of each recording track thus being 1 mm or less). Each site was evaluated with the test stimulus (see previous paragraph). Once a fast site was identified, the electrode's position was held fixed and a response to the experimental stimulus was recorded. If no fast site was found after lowering the electrode to 6 mm below the cortical surface, then lowering was stopped and a slow response was recorded.

The procedure explained in the previous paragraph produced n=90 fast responses and n=78 slow responses, each recorded with a single electrode in a single animal. The set of 90 fast responses exhibits four distinct response types, which we have labeled types 1-4. We developed objective criteria for classifying the type of each fast response: type 1 responses ascend linearly over the entire duration of the 3-s stimulus (objectively $r^2>0.99$, n=38); type 2 responses are not linear (objectively $r^2<0.99$, n=37) but ascend continuously to the end of the stimulus; type 3 responses reach a maximum before the stimulus ends (n=6); type 4 responses are biphasic (n=9).

Data analysis

Statistical analysis of the DA amplitudes measured in fast sites (Fig. 2) was by two-way, mixed factor ANOVA (time after onset of the stimulus (repeated measure) and type as factors) and Bonferroni post-hoc comparisons. Due to unequal sample sizes and variances, one-way ANOVAs were performed at each time point (type as factor) with Games-Howell post-hoc comparisons. Statistical analysis of the correlation of maximum response amplitude and linear clearance rate was by the 2-tailed t-test: the linear clearance rate is the slope of the descending phase of the response where at least five consecutive data points produce a linear response defined by $r^2>0.99$. Statistical analysis of Fig. 3b was by multivariate ANOVA (factors: amplitude and linear clearance rate by type) and Games-Howell post-hoc comparisons. The homogeneity of variance was calculated with Levene's test. Statistical

analysis was performed with IBM SPSS software version 22. Voltammetric color plots were produced in MATLAB.

Kinetic modeling

Quantitative kinetic analysis of the responses was performed with two models composed entirely of first order rate expressions. The first model fits Equation 1 to the ascending phase of the responses:

$$[DA] = At * e^{-k_1 t} + Bt * \left(1 - e^{-k_2 t}\right) \quad \text{Equation 1}$$

and Equation 2 to the descending phase:

$$[DA] = [DA]_i * e^{-k_c t} + C \quad \text{Equation 2}$$

where A and B are release coefficients (μM/s); k_1, k_2, and k_c are first order rate constants (s^{-1}); $[DA]_i$ is the concentration measured at the inflection point of the descending phase of the response; and C is the so-called 'hang-up' concentration (see Results and Discussion for the explanation of hang-up). The two terms on the right hand side of Equation 1, the A and B terms respectively, account separately for the dual nature of the ascending phases of the evoked responses. The exponential decay expression of the A term accounts for short-term depression of the fast responses (types 1-4 - see Results) and the exponential growth expression of the B term accounts for short-term facilitation of the slow response and the type 4 hybrid response. Equation 2 describes DA uptake (after the inflection point) as a first order rate process, with rate constant k_c, that is 'lifted' off its baseline by an amount C.

The second model is a modified version of the restricted diffusion model recently described by Walters *et al*. (2014). The model postulates that the extracellular space is divided into inner and outer compartments, that DA is first released into the inner compartment, and that DA is subsequently transported to the outer compartment where FSCV takes place. The transport step between the compartments represents a generic restricted diffusion mechanism (please see Walters *et al*. 2014 for a detailed discussion of the model and the compartments concept). The modified restricted diffusion model is:

$$\frac{dDA_{ic}}{dt} = R_p \cdot f \cdot e^{-k_R t} - DA_{ic} \cdot k_T \quad \text{Equation 3}$$

$$\frac{d[DA]_{oc}}{dt} = \frac{DA_{ic} \cdot k_T}{V_{oc}} - [DA]_{oc} \cdot k_U \quad \text{Equation 4}$$

where DA_{ic} is the amount (moles) of DA in the inner compartment, $[DA]_{oc}$ is the concentration of DA in the outer compartment, R_p is the amount (moles)of DA released per stimulus pulse, f is the stimulus frequency, k_R is a first order rate constant that modifies DA release, k_T is a first-order rate constant for transport between compartments (identical to the T parameter in Walters *et al*. 2014), V_{oc} is the volume of the outer compartment (arbitrarily set to 16 μm^3, see Walters *et al*. 2014), and k_U is a first-order uptake rate constant. (For clarity of the discussion, we have chosen different subscripts on the rate constants in the two

models.) Kinetic parameters were determined by objective curve fitting (Walters et al., 2014).

Animals: striatal mapping

We implanted n=20 carbon fiber electrodes in the DS of n=10 individual rats (two new electrodes per rat). One of these was implanted in the medial DS (Track A: 1.6 mm anterior to bregma, 1.5 mm lateral from bregma, and 4.5 mm below the cortical surface) and the other in the lateral DS (Track B: 0.2 mm anterior to bregma, 3.8 mm lateral from bregma, and 4.5 mm below the cortical surface, coordinates of (Paxinos and Watson, 1998)). The two electrodes were stereotaxically lowered in 5x200 μm intervals (total track length = 1mm). Each recording site was evaluated with the test stimulus (60 Hz, 250 μA, 200 ms) and the experimental stimulus (60 Hz, 250 μA, 3 s). After the recording session, the electrodes were lowered an additional 500 μm and used to mark the bottom of the track with an electrolytic lesion. Post-mortem histological analysis confirmed that all the electrodes were properly positioned, consistent with their intended stereotaxic target.

RESULTS

Evoked responses in the DS: 4 fast types and 1 slow type

The test stimulus (60 Hz, 250 μA, 200 ms) objectively identified fast responses in n=90 of the 168 individual animals used in the study of kinetic diversity. An evoked response was recorded at each fast site using the experimental stimulus (60 Hz, 250 μA, 3 s). The fast sites exhibit four distinct response types, types 1-4 (Fig. 1: solid lines are the average of multiple responses; the dotted lines are the SEMs; the n values are the number of responses, each recorded from a different animal with a different electrode). The type 4 profile is the one we previously named the hybrid response (Moquin and Michael, 2009): because they respond to the test stimulus, we now classify hybrid responses among the fast types. The type classification is objective: type 1 responses ascend linearly over the entire duration of the 3-s stimulus (objectively, $r^2>0.99$); type 2 responses are not linear (objectively, $r^2<0.99$) but ascend continuously to the end of the stimulus; type 3 responses reach a maximum before the stimulus ends; type 4 responses are biphasic. Slow responses were recorded from the remaining 78 of the 168 animals tested (i.e. those in which we did not identify a fast site). Thus, the DS produces at least 5 distinct evoked responses, 4 fast types and 1 slow type (Fig. 1).

Figure 2 summarizes the type 1-4 DA concentrations at 500 ms intervals during the ascending phase of the response. Statistical analysis was by two-way, mixed factor ANOVA with time (repeated measure) and type as factors (time $F(5,430) = 124.5$, $p<0.00001$; type $F(3,86) = 5.33$, $p<0.005$; interaction $F(15,430) = 14.3$, $p<0.00001$). There were no significant differences between the types at t=0.5 s and t=1.0 s: the types were significantly different thereafter ($p < .02$; Bonferroni post-hoc comparisons). We also performed individual one-way ANOVAs at each time point: there were no significant differences between the types at t=0.5 s and t=1.0 s and the types were significantly different thereafter ($p < .02$; Games-Howell post-hoc comparisons). At t = 1.0 s the type 4 response trends

lower than types 1-3 but this was not significant. Thus, the fast types exhibit similar DA concentrations during the first 1 s of the stimulus and diverge thereafter.

Correlation of DA amplitude with DA clearance

There is a significant linear correlation between the maximum amplitude and linear clearance rate (Fig. 3a: Pearson's correlation coefficient 0.801, 2-tailed t-test $p<0.00001$). Correlations for each type are significant as well (Supporting Information Figure S1). Fig. 3b reports the average values and 95% confidence intervals of the amplitude and linear clearance rate for types 1 and 2 and the slow type (Pearson's correlation coefficient 0.825, 2-tailed t-test, $p<0.00001$): multivariate ANOVA showed that both amplitude ($F(2,149) = 73.2$, $p<0.00001$) and linear clearance rate ($F(2,149) = 36.7$, $p<0.00001$) to be significant. The three types are significantly different in both amplitude and linear clearance rate ($p<0.05$, Games-Howell post-hoc comparisons). Types 3 and 4 were omitted from Fig. 3b because the relatively few number of such types resulted in relatively larger confidence intervals: Supporting Information Figure S2 reports the correlation including types 3 and 4.

The ‘hang-up’

The evoked responses do not return to the pre-stimulus baseline (Fig. 1). Instead, the responses exhibit a consistent ‘hang-up’ feature, which lasts to the end of the recordings sessions (t=10 s). The amplitudes of the hang-up are significant and include a contribution from DA (Supporting Information Figures S3 and S4). For this reason, we proceeded with modeling the responses as-is, i.e. without removing the hang-up feature.

Quantitative kinetic analysis

Equation 1 produces excellent fits to the ascending phase of the evoked responses and Equation 2 produces excellent fits to the descending phase of the evoked responses after their inflection points (Fig. 4, solid lines). In fitting Equation 2 to the descending phase, the DA concentrations at the inflection point and at the end of the recording (at t=10 s, the hang-up) were taken from the data: only k_C was treated as an adjustable parameter. The correlation coefficients for the fits in Figure 4 all exceed 0.99: the high quality of the fits indicates the first-order character of the evoked responses. The parameter values are reported in Table 1 (a dashed entry in Table 1 indicates that the respective parameter was not used for the fit).

The evoked responses exhibit overshoot, i.e. a brief (100-200 ms) continued rise in the DA signal (~100-300 nM) after the stimulus ends. We used the modified restricted diffusion model (Equations 3 and 4) to account for overshoot, using the data between t=0 s and t=4.5 s for curve fitting (Fig. 5 and Table 2). The correlation coefficients of the fits in Fig. 5 all exceed 0.99. Hence, all five DS response types conform to these two first-order kinetic models.

Striatal mapping

We used n=20 individual electrodes to record evoked DA release at six sites along Tracks A and B in the medial and lateral, respectively, DS of n=10 rats. The right panels of Fig. 6 give the location of each recording site and the count of the number of times each site was

classified objectively as fast by means of the test stimulus. Sites along Track A were predominantly slow and sites along Track B were predominantly fast. The left panels of Fig. 6 report averages of the responses at each site (SEMs reported in Supporting Information Figure S5). The responses along Track A are predominantly slow and the profiles along Track B are predominantly type 4. The responses in Fig. 6 were averaged by recording location rather than by type, so they take on a different appearance than those in Fig. 1. A representative example of the response heterogeneity along each track in a single animal is provided in Supporting Information Figure S6. The difference in response amplitudes between Tracks A and B is significant; however, the differences in amplitudes within each track were not significant (Supporting Information Figure S7).

DISCUSSION

Previous reports indicate that pairing of FSCV with electrical stimulation has identified a patchwork of fast and slow DA kinetic domains in the DS (Moquin and Michael, 2009, Wang et al., 2010, Moquin and Michael, 2011, Taylor et al., 2012, Taylor et al., 2013) as well as in the core of the nucleus accumbens (Shu et al., 2013, Shu et al., 2014). We report herein that objectively identified fast domains exhibit 4 distinct evoked responses, types 1-4 (Fig. 1). In addition, the DS exhibits at least one type of slow response. Thus, the DS exhibits at least five distinct responses overall (4 fast types and 1 slow type). Figs. 1-5 comprise 168 recordings performed with 168 individual electrodes in 168 individual animals, which eliminates any possibility that the response diversity stems from the unique properties of any individual electrode or animal. These findings support the conclusion that the recording site is the key determinant of the response type. Neither the fast nor slow responses conform to the expectations of the conventional DA kinetic model (Moquin and Michael, 2009, Taylor et al., 2012, Walters et al., 2014), which assumes a diffusion gap. In contrast, we report here that two new models capture the five response types by suitable adjustments of the first-order kinetic parameters (Tables 1 and 2). A striatal mapping study (Fig. 6) shows that DA's kinetic diversity is selectively expressed in functionally distinct sub-regions of the DS. Overall, this study confirms that a rich but previously unrecognized kinetic diversity exists within the DA terminal field within the DS.

Kinetic diversity contributes to heterogeneity

It is well known that stimulation of DA cell bodies or axons in the midbrain evokes heterogeneous DA responses in the DS and nucleus accumbens (May and Wightman, 1989, Wightman et al., 2007). Our findings extend those prior reports by showing that significant differences exist between the five DS response types. Analysis of the response amplitudes over time (Fig. 2) confirms that the fast types are statistically different beyond t=1.0 s. Correlations of the type in Fig. 3 were previously attributed to variations in local DA innervation density (Stamford et al., 1986, May et al., 1988) but here we show that clustering of the types is also significant. The overall correlation (Fig. 3a) is significant and so too are the correlations for each type (Supporting Information Figure S1). Multivariate analysis (Fig. 3b) confirms that type 1, type 2, and the slow type are statistically different in both amplitude and linear clearance rate: differences with types 3 and 4 did not all reach significance because the relatively few number of such sites contributed to larger confidence

intervals (Supplementary Figure S2). The site clustering suggests that variations in local innervation density occur within each type of response but are not sufficient to explain the numerous significant differences between the types.

Prior literature attributes response heterogeneity to local diffusion effects, such as diffusion barriers or gaps (May and Wightman, 1989, Kawagoe et al., 1992). However, the initial amplitudes of the 4 fast type responses are identical during the first 1 s of the stimulus (Fig. 2). This speaks against any systematic variation in diffusion effects between these sites, because such would strongly influence the initial response rate. All recording sites tested produced an evoked response, so this work does not confirm the previously reported fountain-drain matrix (Rodriguez et al., 2006)

Kinetic analysis

Existing literature suggests that non-DA contaminations of FSCV signals measured after electrical stimulation can be removed via principal component regression (Venton et al., 2003, Heien et al., 2004). We omit principal component regression because, as explained in Supporting Information Figures S3 and S4, the contribution of DA to the post-stimulus hang-ups observed here is clear.

Equations 1 and 2 fit produce excellent fits (correlation coefficients>0.99) to all five DS evoked responses (Fig. 4 and Table 1). Equation 1 captures the linear ascending phase of the type 1 fast response with just the A coefficient. Inclusion of the first order rate expression, e^{-k1t}, captures the downwards curvature of the ascending phase of the type 2 and 3 fast responses, while the alternate expression, $(1 - e^{-k2t}$, captures the upwards curvature of the ascending phase of the slow response. A combination of first-order rate expressions captures the biphasic curvature of the type 4 hybrid response. Beyond their inflection points, the descending phase of the responses exhibit first-order decay but, due to the hang-up, are "lifted off" the baseline. These fits confirm the first-order character of the evoked responses.

Collectively, 16 individual values of the five adjustable parameters (A, B, k_1, k_2, and k_c) capture all five DS profiles (Table 1). The type 1 response requires only two adjustable parameters; hybrid type 4 response requires all five. This stands in contrast to prior reports that DA kinetics are homogeneous in the DS, as expressed by single values of the three kinetic parameters ($[DA]_p$, V_{max}, and K_M) derived from the conventional kinetic model (May et al., 1988, Wightman et al., 1988, Wu et al., 2001). It is important to emphasize that those prior reports focused on optimized responses obtained at recording locations that produce maximal amplitudes with minimal indications of distortion (Kawagoe et al., 1992, Wu et al., 2001). We suggest that optimized responses are the type 1 response reported here. In support of this idea, we note that the value of the A parameter for the type 1 response (Table 1) corresponds to 80 nM DA per stimulus pulse (obtained by dividing A by the 60 Hz stimulus frequency), which is only slightly smaller than typical values of $[DA]_p$ obtained by the prior analysis of optimized responses (Wu *et al*. 2001). However, Equation 1 does not account for diffusion, so it is expected to produce a smaller rate of release. Likewise, the k_C values in Table 1 are smaller than the typical pseudo-first order rate constant of 25 s^{-1} (obtained by dividing a typical value of V_{max}, 5 μM/s, by a typical value of K_M, 0.2 μM).

Evidence is mounting that evoked DA responses conform to the expectations of restricted diffusion (Taylor et al., 2013, Walters et al., 2014). The work of Nicholson and coworkers (Nicholson and Rice, 1991, Hrabetova et al., 2003, Hrabetova and Nicholson, 2004, Tao et al., 2005, Sykova and Nicholson, 2008) shows that diffusion is restricted when molecules enter dead spaces or blocked passageways or become trapped due to binding by molecular recognition or electrostatic interactions: these effects are in addition to the inherent tortuosity of the extracellular space. The model described by Walters *et al*. (2014) represents such restrictions in a generic manner and provides a good fit to evoked responses measured in the DS and nucleus accumbens. The goodness of fit indicates that restricted diffusion offers a plausible explanation for the responses but does not prove that restricted diffusion is the only plausible explanation.

Based on insights provided by Equations 1 and 2, we made two modifications to the restricted diffusion model of Walters *et al*. (2014). The modified model uses only first order rate expressions and includes k_R, which plays a role similar to k_1 and k_2 in Equation 1. The new model uses only 4 adjustable parameters (R_p, k_R, k_T, and k_U), which is one fewer than the diffusion gap model ($[DA]_p$, V_{max}, K_M, the convolution distance, and the diffusion coefficient) and provides excellent fits (correlation coefficients > 0.99) to the ascending phase, the overshoot, and the initial segment of the descending phase of all five response types (Fig. 5). The k_T parameter is the one that accounts for the response overshoot (if k_T were infinitely large there would be no overshoot). The values of k_T in Table 2 fall in a narrow range ($.4 < k_T < 1.0$), which indicates that mass transport differences between recording sites are a minor overall contribution to the heterogeneity of the responses. This lends further support to the concept that the five DS responses reflect DA's kinetic diversity rather than diffusion artifacts. The k_T values in Table 2 are smaller than the dete k_U values, which might indicated that k_T describes the rate rmining step in DA clearance. Consistent with this, we note the similarity between the k_T values in Table 2 and the k_C values in Table 1.

Striatal Mapping

The anatomical organization of the DS includes the patch:matrix compartmentalization and the direct and indirect pathways (for a detailed review, see (Crittenden and Graybiel, 2011)). The patches and matrix receive distinct DA inputs from the substantia nigra pars compacta (SNc), while striatal neurons from the patches (striosomes), but not the matrix, selectively project to the SNc. This provides a basis for anticipating anatomical organization of the DA terminal field as well. Investigators have previously speculated that a relationship might exist between the heterogeneity of evoked DA release and the patch-matrix striatal compartments (May and Wightman, 1989, Rodriguez et al., 2006). Moreover, the medial and lateral sub-regions of the DS are functionally distinct (e.g (Yin et al., 2004, 2005a, Yin et al., 2005b, Yin et al., 2006, Smith and Graybiel, 2014), so it is also relevant to ask if such sub-regions are distinct also with respect to DA kinetic diversity.

Responses recorded along Track A and Track B, located in the medial and lateral sub-regions of the DS, respectively, are distinct in both amplitude and profile (Fig. 6). Kinetic diversity was observed as individual electrodes were moved along each track (see

Supporting Information Figure S6) but, overall, responses along Track A are predominantly slow while those along Track B are predominantly type 4: the difference between, but not within, the tracks is statistically significant (Supporting Information Figure S5 and S7). These findings strongly support the conclusion that DA's kinetic diversity is sub-region dependent. Additional studies will be necessary to identify the specific role of the predominantly slow and predominantly type 4 DA kinetics in the distinct functions of the medial and lateral DS.

CONCLUSION

Even some of the earliest reports on the use of FSCV to record electrically evoked DA release highlighted the heterogeneity of the responses (Stamford et al., 1986, May and Wightman, 1989). Such heterogeneity has been attributed to various forms of distortion (Kawagoe et al., 1992, Wu et al., 2001). In contrast, the present study shows that the various features of the five DS response types can be thoroughly explained with first order rate expressions, which establishes a novel but strong association between response heterogeneity and kinetic diversity of the DS terminal field. This creates a need to consider how kinetic diversity might be related to DA's functional diversity. To that end, our striatal mapping study identified two functionally distinct sub-regions of the DS that exhibit kinetic diversity in a selective manner.

Supplementary Material

Refer to Web version on PubMed Central for supplementary material.

Acknowledgments

This work was financially supported by the NIH (Grants MH 075989, NS 086107).

Abbreviations

DA	dopamine
MFB	medial forebrain bundle
DS	dorsal striatum
FSCV	fast scan cyclic voltammetry

References

Bath BD, Michael DJ, Trafton BJ, Joseph JD, Runnels PL, Wightman RM. Subsecond adsorption and desorption of dopamine at carbon-fiber microelectrodes. Anal Chem. 2000; 72:5994–6002. [PubMed: 11140768]

Brooks DJ. Functional imaging studies on dopamine and motor control. J Neural Transm. 2001; 108:1283–1298. [PubMed: 11768627]

Crittenden JR, Graybiel AM. Basal ganglia disorders associated with imbalances in the striatal striosome and matrix compartments. Front Neuroanat. 2011:5. [PubMed: 21369363]

de la Fuente-Fernandez R, Schulzer M, Kuramoto L, Cragg J, Ramachandiran N, Au WL, Mak E, McKenzie J, McCormick S, Sossi V, Ruth TJ, Lee CS, Calne DB, Stoessl AJ. Age-Specific

Progression of Nigrostriatal Dysfunction in Parkinson's Disease. Ann Neurol. 2011; 69:803–810. [PubMed: 21246604]

Ewing AG, Bigelow JC, Wightman RM. Direct in vivo monitoring of dopamine released from two striatal compartments in the rat. Science. 1983; 221:169–171. [PubMed: 6857277]

Grace AA. Phasic versus tonic dopamine release and the modulation of dopamine system responsivity: A hypothesis for the etiology of schizophrenia. Neuroscience. 1991; 41:1–24. [PubMed: 1676137]

Heien M, Johnson MA, Wightman RM. Resolving neurotransmitters detected by fast-scan cyclic voltammetry. Anal Chem. 2004; 76:5697–5704. [PubMed: 15456288]

Hrabetova S, Hrabe J, Nicholson C. Dead-space microdomains hinder extracellular diffusion in rat neocortex during ischemia. J Neurosci. 2003; 23:8351–8359. [PubMed: 12967997]

Hrabetova S, Nicholson C. Contribution of dead-space microdomains to tortuosity of brain extracellular space. Neurochem Int. 2004; 45:467–477. [PubMed: 15186912]

Hull EM, Lorrain DS, Du J, Matuszewich L, Lumley LA, Putnam SK, Moses J. Hormone-neurotransmitter interactions in the control of sexual behavior. Behav Brain Res. 1999; 105:105–116. [PubMed: 10553694]

Kawagoe KT, Garris PA, Wiedemann DJ, Wightman RM. Regulation of transient dopamine concentration gradients in the microenvironment surrounding nerve terminals in the rat striatum. Neuroscience. 1992; 51:55–64. [PubMed: 1465186]

Kim J-H, Son Y-D, Kim H-K, Lee S-Y, Cho S-E, Kim Y-B, Cho Z-H. Antipsychotic-Associated Mental Side Effects and Their Relationship to Dopamine D(2) Receptor Occupancy in Striatal Subdivisions A High-Resolution PET Study With (11)C Raclopride. J Clin Psychopharmacol. 2011; 31:507–511. [PubMed: 21694619]

Kuhr WG, Ewing AG, Caudill WL, Wightman RM. Monitoring the stimulated release of dopamine with in vivo voltammetry. I: Characterization of the response observed in the caudate nucleus of the rat. J Neurochem. 1984; 43:560–569. [PubMed: 6736965]

May LJ, Kuhr WG, Wightman RM. Differentiation of dopamine overflow and uptake processes in the extracellular fluid of the rat caudate nucleus with fast-scan in vivo voltammetry. J Neurochem. 1988; 51:1060–1069. [PubMed: 2971098]

May LJ, Wightman RM. Heterogeneity of stimulated dopamine overflow within rat striatum as observed with in vivo voltammetry. Brain Res. 1989; 487:311–320. [PubMed: 2786444]

Michael DJ, Wightman RM. Electrochemical monitoring of biogenic amine neurotransmission in real time. J Pharm Biomed Anal. 1999; 19:33–46. [PubMed: 10698566]

Moquin KF, Michael AC. Tonic autoinhibition contributes to the heterogeneity of evoked dopamine release in the rat striatum. J Neurochem. 2009; 110:1491–1501. [PubMed: 19627437]

Moquin KF, Michael AC. An inverse correlation between the apparent rate of dopamine clearance and tonic autoinhibition in subdomains of the rat striatum: a possible role of transporter-mediated dopamine efflux. J Neurochem. 2011; 117:133–142. [PubMed: 21244425]

Nicholson, C.; Rice, ME. Diffusion of ions and transmitters in the brain cell microenvironment.. In: Fuxe, K.; Agnati, LF., editors. Volume Transmission in the Brain. Raven Press; New York: 1991. p. 279-294.

Pappata S, Salvatore E, Postiglione A. In vivo imaging of neurotransmission and brain receptors in dementia. J Neuroimaging. 2008; 18:111–124. [PubMed: 18380693]

Paxinos, G.; Watson, C. The Rat Brain in Stereotaxic Coordinates. Academic Press; New York, NY: 1998.

Pellegrino, LJ.; Pellegrino, AS.; Cushman, AJ. A Stereotaxic Atlas of the Rat Brain. Plenum Press; New York, NY: 1979.

Rodriguez M, Morales I, Gomez I, Gonzalez S, Gonzalez-Hernandez T, Gonzalez-Mora JL. Heterogeneous Dopamine Neurochemistry in the Striatum: The Fountain-Drain Matrix. J Pharmacol Exp Ther. 2006; 319:31–43. [PubMed: 16825531]

Schultz W. Multiple dopamine functions at different time courses. Annu Rev Neurosci. 2007; 30:259–288. [PubMed: 17600522]

Shu Z, Taylor IM, Michael AC. The dopamine patchwork of the rat nucleus accumbens core. Eur J Neurosci. 2013; 38:3221–3229. [PubMed: 23937532]

Shu Z, Taylor IM, Walters SH, Michael AC. Region-and domain-dependent action of nomifensine. Eur J Neurosci. 2014; 40:2320–2328. [PubMed: 24766210]

Smith KS, Graybiel AM. Investigating Habits: Strategies, Technologies, and Models. Front Behav Neurosci. 2014; 8

Stamford JA, Kruk ZL, Millar J. In vivo voltammetric characterization of low affinity striatal dopamine uptake: Drug inhibition profile and relation to dopaminergic innervation density. Brain Res. 1986; 373:85–91. [PubMed: 3487373]

Stamford JA, Kruk ZL, Millar J. Stimulated limbic and striatal dopamine release measured by fast cyclic voltammetry: anatomical, electrochemical and pharmacological characterisation. Brain Res. 1988; 454:282–288. [PubMed: 3261616]

Sykova E, Nicholson C. Diffusion in brain extracellular space. Physiol Rev. 2008; 88:1277–1340. [PubMed: 18923183]

Tao A, Tao L, Nicholson C. Cell cavities increase tortuosity in brain extracellular space. J Theor Biol. 2005; 234:525–536. [PubMed: 15808873]

Taylor IM, Ilitchev AI, Michael AC. Restricted Diffusion of Dopamine in the Rat Dorsal Striatum. ACS Chem Neurosci. 2013; 4:870–878. [PubMed: 23600442]

Taylor IM, Jaquins-Gerstl A, Sesack SR, Michael AC. Domain-dependent effects of DAT inhibition in the rat dorsal striatum. J Neurochem. 2012; 122:283–294. [PubMed: 22548305]

Urban NL, Slifstein M, Meda S, Xu X, Ayoub R, Medina O, Pearlson G, Krystal J, Abi-Dargham A. Imaging human reward processing with positron emission tomography and functional magnetic resonance imaging. Psychopharmacology (Berl). 2012; 221:67–77. [PubMed: 22052081]

Venton BJ, Michael DJ, Wightman RM. Correlation of local changes in extracellular oxygen and pH that accompany dopaminergic terminal activity in the rat caudate-putamen. J Neurochem. 2003; 84:373–381. [PubMed: 12558999]

Wagner AK, Sokoloski JE, Ren D, Chen X, Khan AS, Zafonte RD, Michael AC, Dixon CE. Controlled cortical impact injury affects dopaminergic transmission in the rat striatum. J Neurochem. 2005; 95:457–465. [PubMed: 16190869]

Walters SH, Taylor IM, Shu Z, Michael AC. A Novel Restricted Diffusion Model of Evoked Dopamine. ACS Chem Neurosci. 2014

Wang YX, Moquin KF, Michael AC. Evidence for coupling between steady-state and dynamic extracellular dopamine concentrations in the rat striatum. J Neurochem. 2010; 114:150–159. [PubMed: 20403079]

Wightman RM, Amatore C, Engstrom RC, Hale PD, Kristensen EW, Kuhr WG, May LJ. Real-time characterization of dopamine overflow and uptake in the rat striatum. Neuroscience. 1988; 25:513–523. [PubMed: 3399057]

Wightman RM, Heien MLAV, Wassum KM, Sombers LA, Aragona BJ, Khan AS, Ariansen JL, Cheer JF, Phillips PEM, Carelli RM. Dopamine release is heterogeneous within microenvironments of the rat nucleus accumbens. Eur J Neurosci. 2007; 26:2046–2054. [PubMed: 17868375]

Wu Q, Reith MEA, Wightman RM, Kawagoe KT, Garris PA. Determination of release and uptake parameters from electrically evoked dopamine dynamics measured by real-time voltammetry. J Neurosci Methods. 2001; 112:119–133. [PubMed: 11716947]

Yin HH, Knowlton BJ, Balleine BW. Lesions of dorsolateral striatum preserve outcome expectancy but disrupt habit formation in instrumental learning. Eur J Neurosci. 2004; 19:181–189. [PubMed: 14750976]

Yin HH, Knowlton BJ, Balleine BW. Blockade of NMDA receptors in the dorsomedial striatum prevents action–outcome learning in instrumental conditioning. Eur J Neurosci. 2005a; 22:505–512. [PubMed: 16045503]

Yin HH, Knowlton BJ, Balleine BW. Inactivation of dorsolateral striatum enhances sensitivity to changes in the action–outcome contingency in instrumental conditioning. Behav Brain Res. 2006; 166:189–196. [PubMed: 16153716]

Yin HH, Ostlund SB, Knowlton BJ, Balleine BW. The role of the dorsomedial striatum in instrumental conditioning. Eur J Neurosci. 2005b; 22:513–523. [PubMed: 16045504]

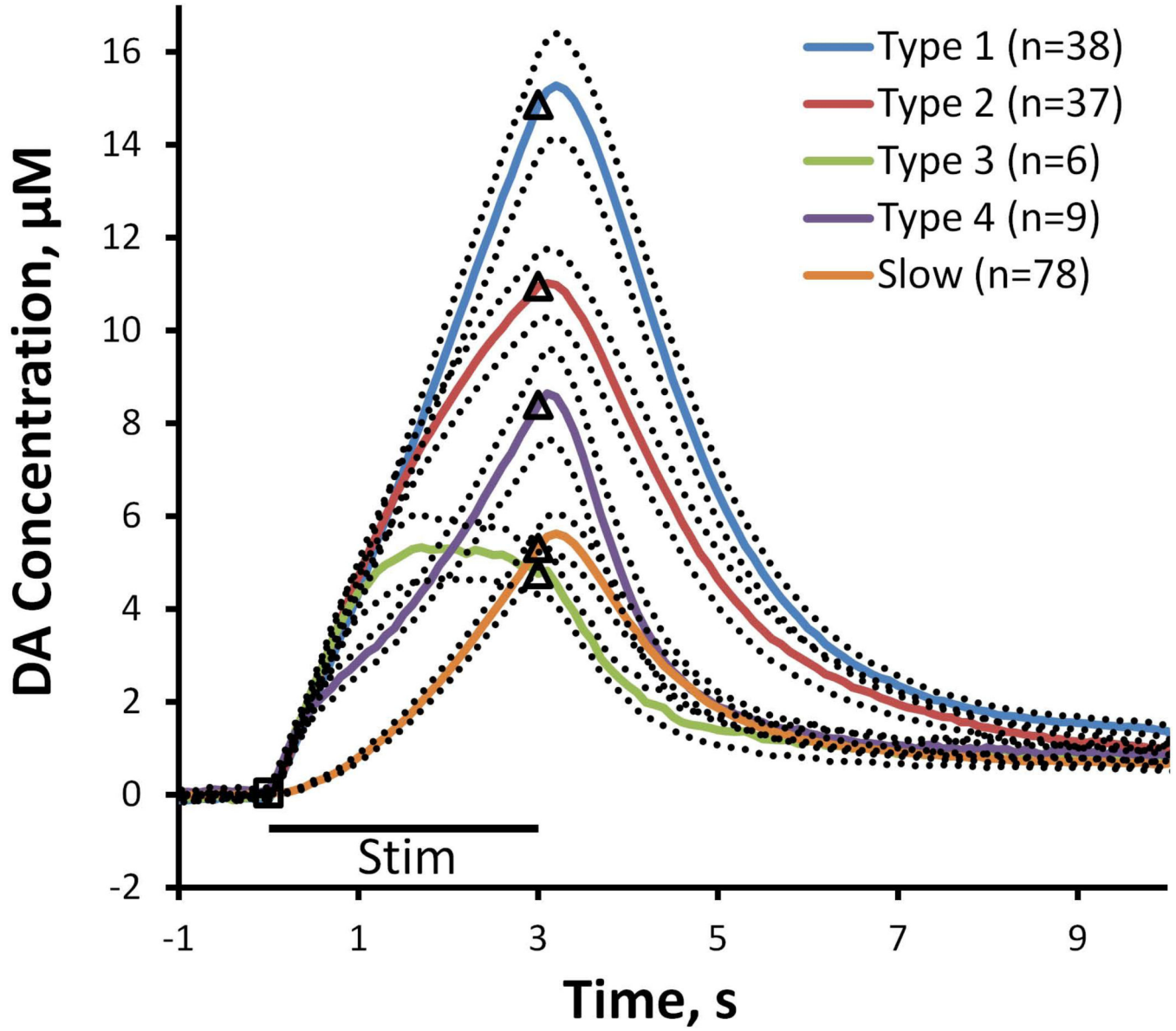

Figure 1.

The five DS responses (Type 1 in blue, Type 2 in red, Type 3 in green, Type 4 in purple, Slow in orange). The solid lines are the averages of the responses and the dotted lines are the SEMs: the n values are listed on the figure. The black bar below the curves denotes the duration of MFB stimulation (black square indicates the onset of stimulation and the black triangles mark the end of the stimulus).

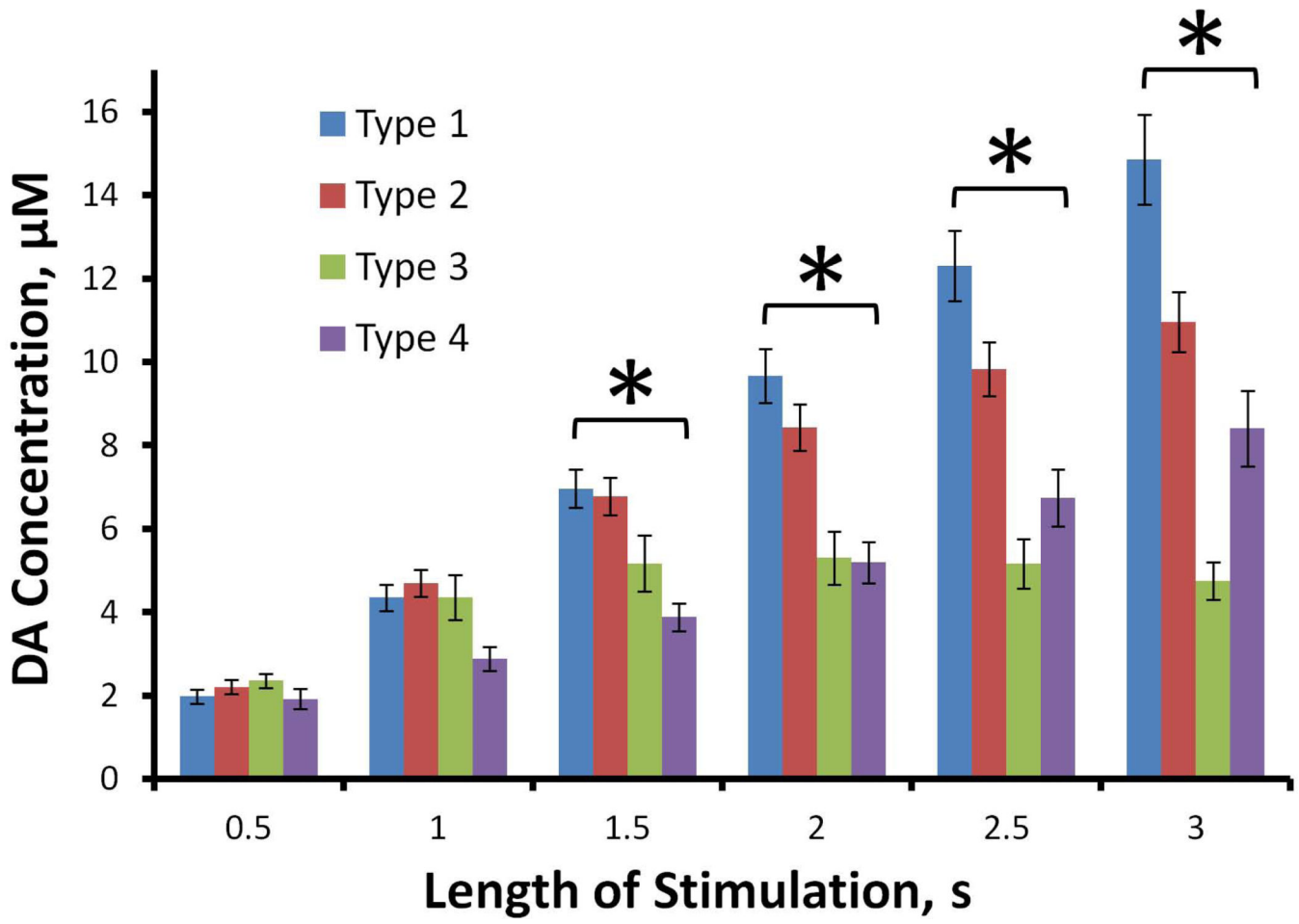

Figure 2.

The evoked DA concentrations (mean ± SEM, n as reported in Fig. 1) at 500 ms intervals (2-way, mixed model ANOVA with time (the repeated measure) and type as factors: type $F(3,86) = 5.33$, $p<0.005$); time $F(5,430) = 124.5$, $p<0.00001$; interaction $F(15,430) = 14.3$, $p<0.00001$). Bonferroni post-hoc comparisons: differences among types were significant at t = 1.5 to 3 s (*$p<0.02$) but not before.

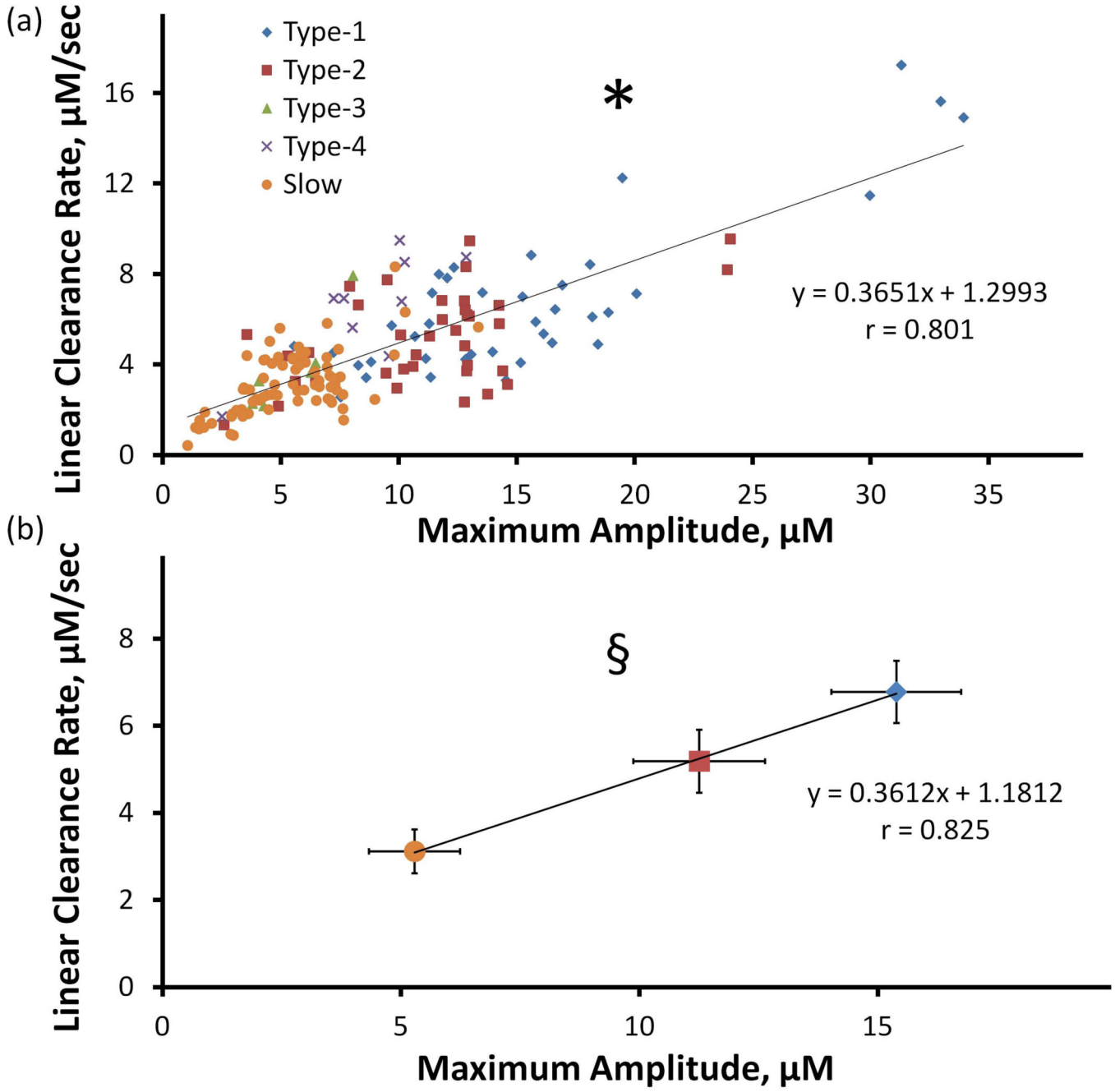

Figure 3.

a) Correlation of maximum amplitude and linear clearance rate of evoked response in the DS (* Pearson's correlation coefficient 0.801; paired-sample 2-tailed t-test $p<0.00001$). b) Correlation of the average values of amplitude and linear clearance rate (± 95% confidence intervals) of types 1, 2, and slow (§ Pearson's correlation coefficient 0.825; paired-sample 2-tailed t-test $p<0.00001$: multivariate ANOVA; amplitude $F(2,149) = 73.2$, $p<0.00001$, linear clearance rate $F(2,149) = 36.7$, $p<0.00001$). All individual maximum amplitudes and linear clearance rates are significantly different ($p<0.05$, Games-Howell post-hoc comparisons).

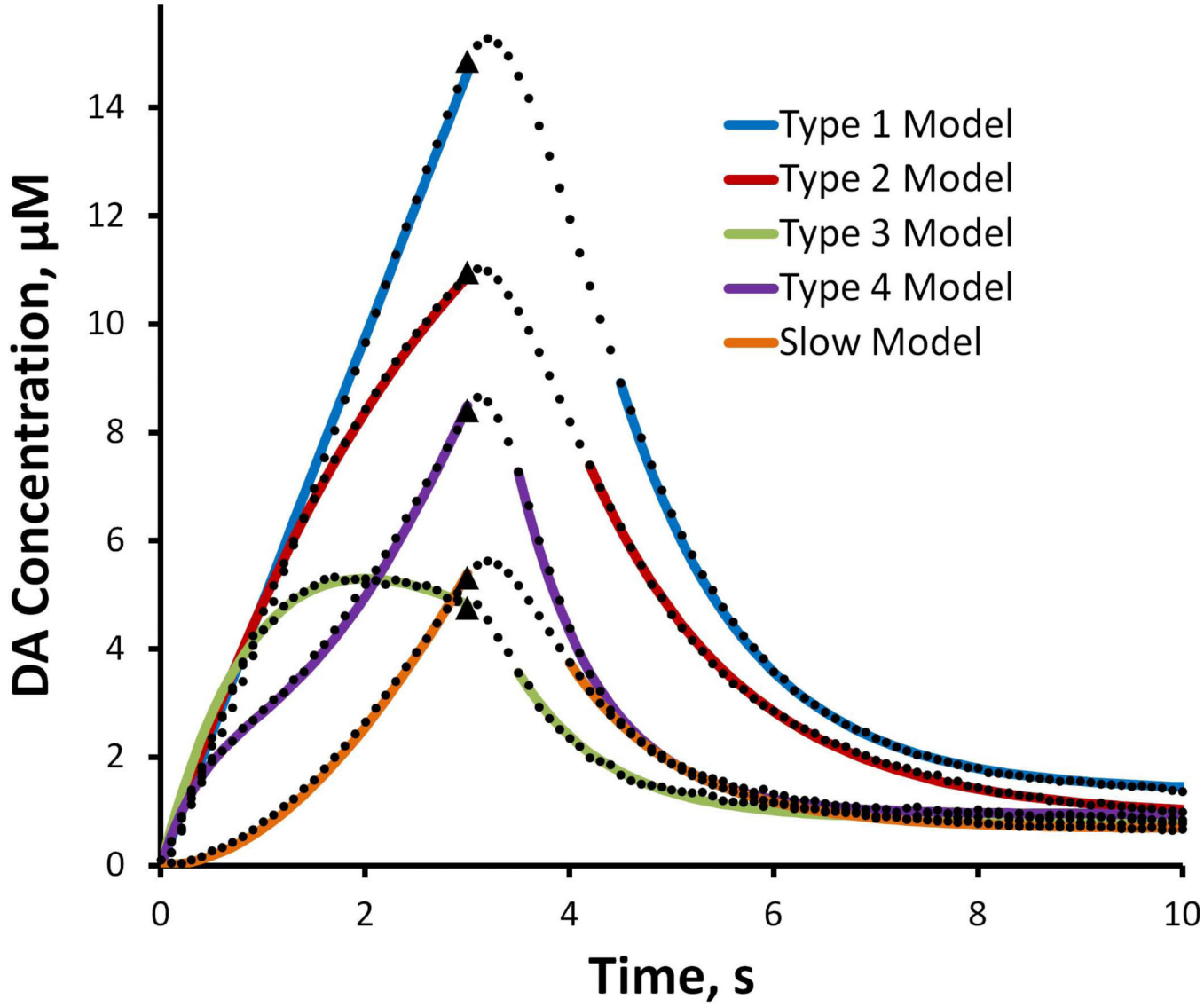

Figure 4.

The means of the 5 response types from the rat DS (black dots, SEMs omitted for clarity) and the model fits (solid lines) obtained with Equations 1 and 2 of the text (Equation 1 fits the ascending phase of the response and Equation 2 fits the descending phase of the response). The correlation coefficients for all fits exceed 0.99. The parameters are reported in Table 1. The stimulus begins at t = 0 s and ends at t = 3 s (black triangles).

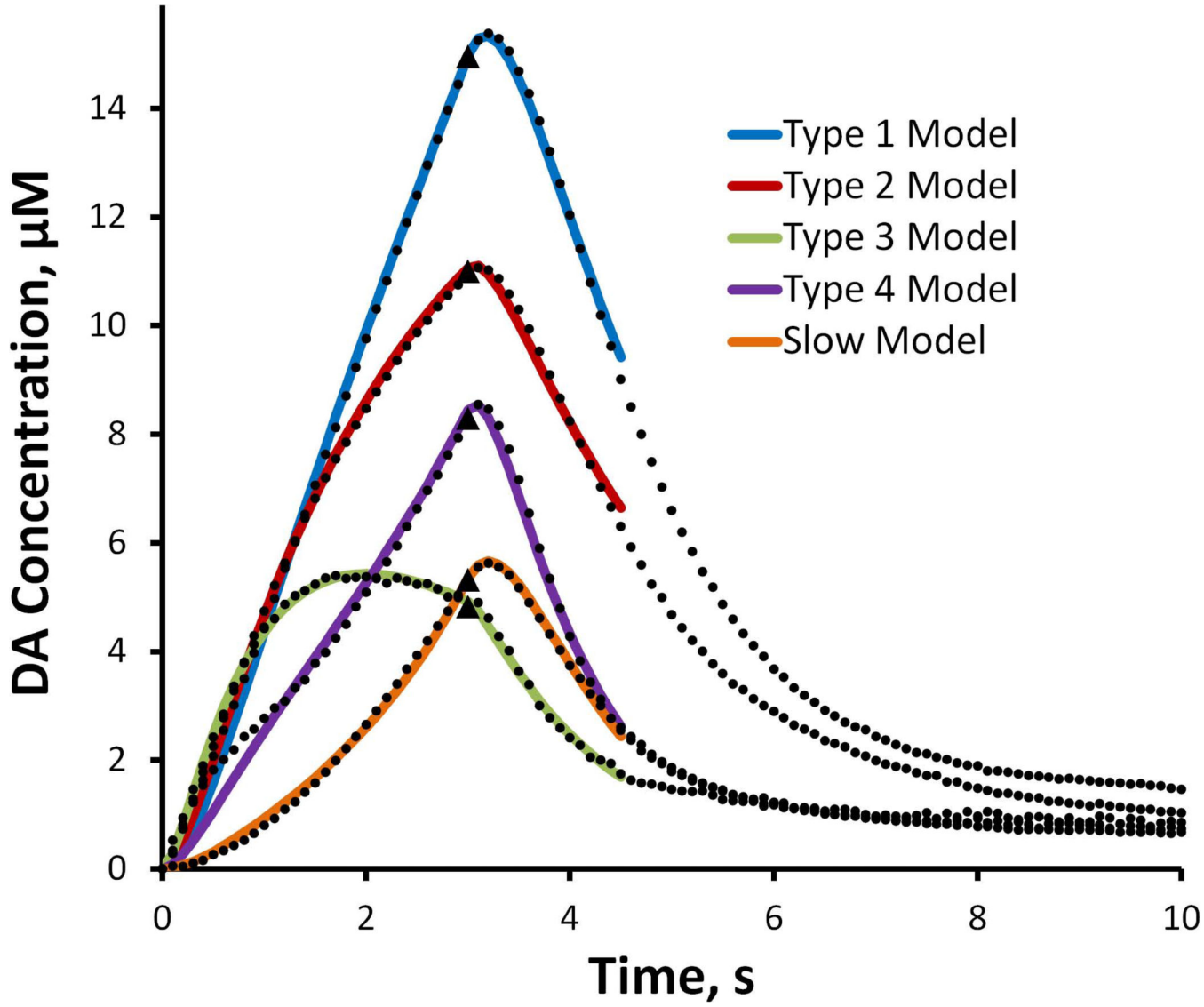

Figure 5.

The mean of the 5 response types from the rat DS (black dots, SEMs omitted for clarity) and the model fits (solid lines) obtained with Equations 3 and 4 of the text. The correlation coefficients for all fits exceed 0.99. The parameters are reported in Table 2. The stimulus begins at t = 0 s and ends at t = 3 s (black triangles).

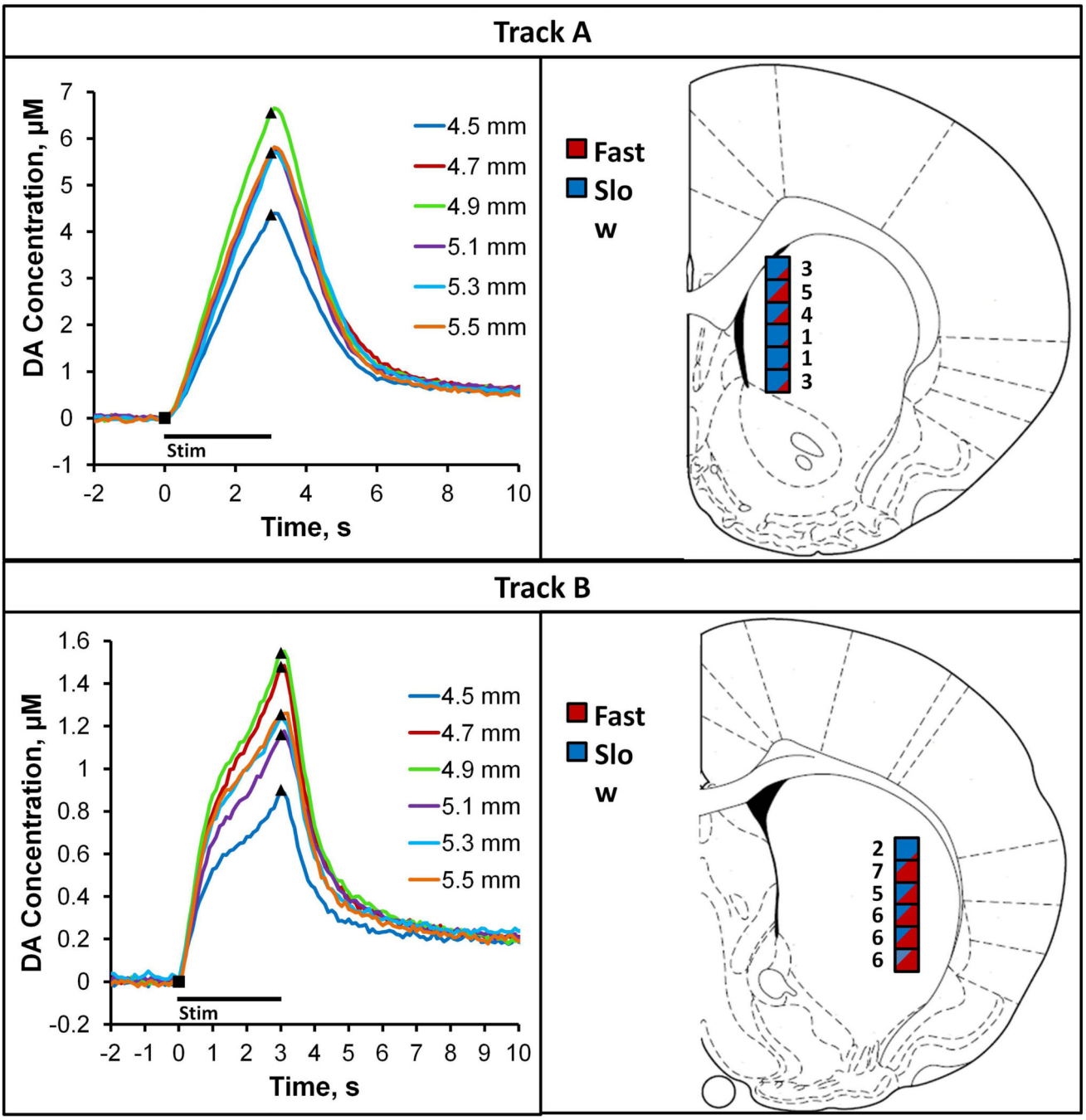

Figure 6.

Striatal mapping along Track A (top) and Track B (bottom). Right Panels: the boxes show the anatomical location of each recording site and the number of fast responses observed at each location (red represents fast and blue represents slow). Left Panels: average of the responses long Track A and Track B (n=10 electrodes per track, 1 track each per rat; SEMS reported in Supplementary Figure S5).

Table 1

Parameters for the model fits in Fig. 4. The parameters are defined in Equations 1 and 2 of the text. A dashed entry indicates that the respective parameter was not used to fit the respective type.

	A (μM/s)	B (μM/s)	k_1 (s^{-1})	k_2 (s^{-1})	k_c (s^{-1})
Type 1	4.9	-	-	-	0.82
Type 2	5.6	-	0.145	-	0.69
Type 3	7.2	-	0.5	-	1.1
Type 4	6	5.4	1.25	0.23	1.2
Slow	-	5.4	-	0.135	0.92

Table 2

Parameters for the model fits in Fig. 5. The parameters are defined in Equations 3 and 4 of the text.

	R_p (mols×10^{21})	k_r (s^{-1})	k_t (s^{-1})	k_u (s^{-1})
Type 1	13.1	−.24	.47	3.4
Type 2	25.3	.002	.40	5.5
Type 3	24.9	.35	.76	8.4
Type 4	4.6	−.41	1.0	4.3
Slow	1.3	−.67	.85	2.9